ISSN 2079-1704. Хімія, фізика та технологія поверхні. 2025. Т. 16. № 3. С. 385-405

PACS: 07.20.Hy; 65.60.+a; 68.60.Dv; 28.52.Cx; 28.41.Bm; 89.30. g; 81.70. Pg doi: 10.15407/hftp16.03.385

V.V. Pidlisnyuk [1], T.R. Stefanovska [2], L.I. Borysenko [3], V.P. Klius [4], H.O. Chetveryk [4], A.I. Medkov [2, 5], V.V. Lisnyak [3]

INFLUENCE OF THE INITIAL BIOMASS STATE AND PYROLYSIS CONDITIONS ON THE PROPERTIES OF BIOCHAR PRODUCED FROM *MISCANTHUS* × *GIGANTEUS* WASTE

[1] Department of the Environmental Chemistry and Technology, Faculty of Environment, Jan Evangelista Purkynĕ University
15, Pasterova, 400 96, Usti nad Labem, Czech Republic
[2] Department of Entomology, Faculty of Plant Protection, Biotechnologies and Ecology
National University of Life and the Environmental Sciences
15 Heroiv oborony Str., 03041, Kyiv, Ukraine
[3] Chuiko Institute of Surface Chemistry of National Academy of Sciences of Ukraine
17 Oleg Mudrak Str., Kyiv, 03164, Ukraine, E-mail: lisnyak@nas.gov.ua
[4] Institute of Renewable Energy of National Academy of Sciences of Ukraine
20-a Hnata Hotkevicha Str., 02094, Kyiv, Ukraine
[5] Department of Agrobioresources and Environmentally Safe Technologies
Institute of Agroecology and Environmental Management
12 Metrologichna Str., Kyiv, 03143, Ukraine

The influence of pyrolysis conditions and the initial biomass state of Miscanthus x giganteus on the properties of biochar as a final product of oxidative and dry pyrolysis was investigated. Miscanthus biomass chips and waste pellets as well as wood waste were tested as feedstocks. Miscanthus chips were obtained from biomass grown on agricultural or marginal soils. The feedstocks were processed into biochar by oxidative pyrolysis in specially designed "household" and "farmer's" stoves and by dry pyrolysis in a muffle furnace. Higher pyrolysis temperatures (600–700 °C) resulted in biochar with higher specific surface area (SSA) but lower yield. A balance between yield and SSA was found at 600 °C for 30–40 minutes, making this condition ideal for high-porosity biochar suitable for adsorption applications. For soil improvement, oxidative pyrolysis biochar from Miscanthus pellets and wood waste is preferred due to its higher fixed carbon content. For adsorption-based applications, dry pyrolysis biochar from Miscanthus chips is better due to its higher SSA. For fuel applications, biochar from oxidative pyrolysis of wood waste and Miscanthus waste pellets are ideal due to the highest calorific values. Thermogravimetric analysis of Miscanthus chips heated in air showed a process involving dehydration, pyrolysis, and oxidation reactions, and revealed its stages, namely, dehydration at 50–140 °C, hemicellulose degradation at 230–360 °C, cellulose degradation at 285–380 °C, and slow lignin destruction at 200–700 °C. Miscanthus chips exhibit spontaneous combustion characteristics, with smoldering beginning at 204 °C and complete combustion at 333 °C. Biochars produced from Miscanthus feedstocks has lower dehydration temperatures than corresponding Miscanthus feedstock, and it loses 86.2–92 % of its weight during thermal processing. Biochar obtained from Miscanthus pellets has the highest moisture content, while biochar from Miscanthus chips is less hydrophilic. Thermal stability varies among biochar samples, with significant differences in weight loss patterns during pyrolysis and oxidation. These differences suggest structural variations, likely due to the feedstock composition and pyrolysis conditions. Prepared biochar has both hydrophobic and hydrophilic properties, which is confirmed by the presence of characteristic peaks of hydrophobic and hydrophilic groups in the FTIR spectra. In particular, FTIR spectroscopy indicates the presence of hydroxyl (–OH), carbonyl (C=O), carboxyl (–COOH), and methylene (CH_2) groups in carbonization products derived from the structural components of biomass – cellulose, hemicellulose and lignin. It was found that the SSA values of biochar from Miscanthus pellets produced by oxidative pyrolysis and biochar from chips produced by dry pyrolysis are in accordance with the parameters recommended by the International Biochar Initiative and are 187 and 419 m^2/g, respectively. It has been concluded that the production of biochar from Miscanthus pellets by oxidative pyrolysis requires minimal energy consumption per unit of product. Processing Miscanthus waste by converting it into biochar is a promising solution within the circular economy concept, as biochar derived from Miscanthus × giganteus can be an effective additive that can help restore degraded soils through phytoremediation.

***Keywords**: Miscanthus chips and pellets, oxidative pyrolysis, dry pyrolysis, processing temperature, specific surface area of biochar*

© V.V. Pidlisnyuk, T.R. Stefanovska, L.I. Borysenko, V.P. Klius, H.O. Chetveryk, A.I. Medkov, V.V. Lisnyak, 2025

INTRODUCTION

Biochar is a carbon-rich solid fraction produced during the thermal decomposition of biomass under oxygen-free or oxygen-limited conditions in the temperature range of 300–800 °C [1–3]. When applied to soil, biochar can increase soil carbon uptake and potentially reduce carbon dioxide emissions [4, 5]. When used as a soil fertilizer, biochar can improve soil structure and composition, increase water holding capacity, and ensure nutrient availability in the soil [5]. Typically, the use of biochar stimulates microbial activity, which accelerates the decomposition of nutrients accumulated on the surface and in the volume of biochar and prevents their loss through leaching; biochar use generally affects soil biota by altering the composition of the microbial biome and the functional activity of the microbial cenosis [6]. The main factors influencing the properties of biochar are the type of feedstock (wood and crop residues) and the temperature and time of processing of the feedstock during pyrolysis [7]. As a result of the Russian-Ukrainian war, Ukraine's soils have been severely damaged [8, 9], therefore, soil restoration is an important task for the post-war development of the country. A promising way to restore degraded soils in Ukraine is the cultivation of a perennial plant (*Miscanthus* × *giganteus*), a C4 energy crop used for phytoremediation of slightly contaminated and/or marginal soils and for soil carbon sequestration [10, 11].

This crop can increase soil organic carbon due to the presence of a developed root structure inherent to perennial crops. However, when *Miscanthus* × *giganteus* is grown on contaminated soils, the associated waste biomass, e.g., contaminated roots, and the total biomass of the first two years of vegetation must be utilized, here pyrolysis of *Miscanthus* waste can be a promising solution to this problem [11]. The biochar obtained from waste pyrolysis can be used in the next growing cycle of this crop, thus ensuring a circular economic approach: resource recovery [11, 12].

In the world [13, 14], biochar is mainly produced from wood waste, while the production of biochar from plant materials, e.g. cereal straw, corn stalks, sunflowers, energy crops, is being developed and intensified [15]. However, currently in Ukraine the use of plant material for biochar, bio-oil or syngas production is in the initial stage and mainly focused on the level of laboratory research [16].

Up to the present time, numerous studies have dealt with biochar production, see for example in Refs. [17–19]; however, considerable attention should be paid to specific cases [20, 21], including pyrolysis technologies, which have been adopted in Ukraine and typically work with pyrolysis of biomass waste in a dense layer [22–24]. Pyrolysis technologies are formally described in the Ukrainian standard "Synthetic Fuel. Terms and Definitions" DSTU 7502:2014 [25], and it defines pyrolysis as the irreversible thermal decomposition of fuel in the absence of or with limited access to air.

Earlier technical literature [26, 27] described the process of dry pyrolysis, historically known as destructive distillation or dry distillation of wood. In this process, organics, biomass, or other carbonaceous materials are heated with limited air access, with dry or low moisture feedstock, and without added solvents. Under these conditions, the organic material of the feedstock undergoes thermal decomposition, producing char (a solid, carbon-rich residue), bio-oil (a condensable liquid fraction), and non-condensable pyrolysis gases. Dry pyrolysis typically operates at temperatures between 500 and 900 °C, or between 300 and 800 °C, with heating rates up to 50 °C min^{-1} and residence times ranging from tens of minutes to several hours, depending on the reactor design and the target product [28, 29]. The solid residue produced is often referred to as a coke–ash mixture, containing the fixed carbon content of the original feedstock. The gaseous products are typically high calorific and nitrogen-free pyrolysis gases containing hydrogen (H_2), carbon monoxide (CO), methane (CH_4) and other light hydrocarbons [30, 31].

Traditionally, dry pyrolysis of wood has been the dominant method for char production, with significant yields and the production of tar-like compounds that have been used by civilizations for millennia [26, 27]. It remains the most installed process for high-yield biochar production, although it can be operated to produce multiple products (e.g., oil and gas) in addition to char [21, 26–28]. In addition to biochar, dry pyrolysis of wood—often referred to as wood distillation—yields valuable commodity chemicals, including methanol, acetic acid, and acetone [27, 31, 32]. Moderate heating rates with long residence times (slow or intermediate

pyrolysis) yield high amounts of gases and vapors of 30–35 % [28] and about 20–40 % as char [29]. In the early 1900s [26, 27], destructive distillation of wood was widely practiced on a commercial scale, using retorts to heat the wood and extract valuable by-products. In modern applications, dry pyrolysis is typically performed in closed kilns or retorts [30, 31], where non-condensable gases are often recycled to fuel the reactor itself, improving the overall energy efficiency of the process.

Typically, dry pyrolysis refers to a process in which material is exposed to high temperatures without the presence of added moisture or a liquid phase [20], a condition that significantly influences the nature and composition of the resulting products [32–34]. This is in contrast to other pyrolysis methods, which may involve some moisture or liquid catalysts [17]. In the absence of a solvent [28, 29], the thermal cleavage of covalent bonds in biomass is driven by heat alone. This thermolysis produces extractable compounds that remain trapped within the solid particle matrix. Although this bond cleavage mechanism is similar to that of liquefaction [19], the absence of a solvent phase prevents the transport of these liberated compounds away from the solid structure [33]. As a result, tar precursors accumulate within the heated particles, with only a small fraction escaping by evaporation. These trapped intermediates exhibit remarkable thermal stability, persisting at 400 °C for up to 120 seconds or more without significant decomposition [20]. This retention of reactive intermediates distinguishes dry pyrolysis from solvent-based liquefaction, where such compounds can be rapidly extracted and further transformed in the liquid phase.

Dry pyrolysis can be performed in a low-oxygen atmosphere, which prevents combustion while allowing thermal degradation [34, 35]. Because dry pyrolysis is commonly used to produce carbon-rich materials [35], and no liquid or moisture is added, the process relies solely on heat to degrade the biomaterials, and the process typically lasts between 300 and 900 °C for hours to minutes [36].

Although both dry and wet pyrolysis involve similar molecular degradation processes in which macromolecules are broken down into liquid and gaseous products, the presence or absence of moisture significantly affects the properties of the resulting biochar [20, 37, 38]. Solid-solid interactions in dry pyrolysis result in greater structural rearrangements, and studies have shown that biochar from dry pyrolysis tends to be more thermally stable than that from wet pyrolysis [20, 37].

In summary, dry pyrolysis is a solvent-free process that may be ideal for producing biochar from dry, low-moisture feedstocks such as wood and agricultural waste [35, 36, 38]. The efficiency of the process and the quality of the resulting product depend on factors such as feedstock type, temperature, and residence time, so experimental optimization is essential to achieve the best results.

Pyrolysis is not always carried out in an atmosphere where there is no oxidant as such, currently there are many studies describing the results of the application of oxidative pyrolysis, there are reviewed in [39, 40], to obtain biochar, synthesis gas and H_2 [41–43]. Practical examples of oxidative pyrolysis are smoldering or pyrolysis in an oxidizing environment as a sub-process of gasification [44–46]. Smoldering is known to be a slow, low-temperature, flameless form of combustion supported by heat, which is released in particular when oxygen comes into direct contact with the solid fuel surface [44], as for pellets and similar bio-feedstocks. Smoldering is critical because, if the process is controlled, it allows the production of biochar with low or even no energy consumption [47, 48]. Today, there are many reports devoted to industrial and portable fixed-bed combustors of a pelleted biomass [49, 50], downdraft continuous fixed bed reactors [51, 52], which are used to carbonize biomass by autothermal oxidative pyrolysis in fixed bed carbonization units [53] and biomass downdraft gasifier engine systems [54] designed for biomass gasification, pyrolysis, and torrefaction in order to obtain biochar and energy [55, 56].

From canonic consideration [57, 58], oxidative pyrolysis process is composed of drying, high temperature pyrolysis, partial oxidation, and reduction. This method should not be confused with the simple burning/combustion where the temperature is not so high as for pyrolysis, 190 versus 300 °C [59]. So, it can be defined as a partial oxidation through indirect combustion of the biomass in presence of a limited oxidant. The outputs in the form of flue gas are generally termed as fuel gas in the form of “producer gas” or “syngas” [58, 59].

In summary, oxidative pyrolysis is an irreversible thermal decomposition process in which biofuel partially combusts with limited air access while directly interacting with pyrolysis gas. The byproducts of oxidative pyrolysis are coke ash residue and low-calorie pyrolysis gas. Indeed, oxidative pyrolysis is usually the first step in a two-stage gasification process, as the initial sub-process is autothermal [48, 53]. Furthermore, in downdraft gasification, when the air intake is at the top, oxidative pyrolysis occurs in this region.

Today, there are different gasification variants (downflow and upflow), in which the placement of the air inlet determines where in the reactor the oxidative pyrolysis takes place [54]. One variant operates under the condition of a downward air supply, which we used in the presented work. Pyrolysis stove designs are classified according to whether they operate in batches or continuously and according to the size and volume of the raw materials processed into biochar. Consequently, these stoves range from compact, portable household models [60] to large industrial ones [61–63].

In light of recent developments in dry and wet pyrolysis technologies, we employed a custom-built, pilot-scale reactor system in this study. This system allows for controlled experimentation under oxidative pyrolysis. We also adapted the dry pyrolysis technique for *Miscanthus* × *giganteus* biomass conversion to bridge the gap between lab-scale studies and practical, scalable applications. Below, we report our attempts to process *Miscanthus* × *giganteus* waste biomass into biochar effectively by oxidative and dry pyrolysis under optimal conditions.

EXPERIMENTAL

Materials. The starting materials used in the study were (i) *Miscanthus* chips from *Miscanthus* × *giganteus* biomass grown on agricultural soil in the experimental field of Ternopil Volodymyr Hnatiuk National Pedagogical University; the GPS coordinates are 49.5418397 N, 25.568175 E., (hereinafter referred to as *Miscanthus* chips 1), (ii) chips produced from *Miscanthus* × *giganteus* biomass grown on marginal soil from Croatia (hereinafter referred to as miscanthus chips 2), and (iii) *Miscanthus* pellets produced by Pellegrin LLC (Vinnytsia region) from *Miscanthus* × *giganteus* waste.

Oxidative Pyrolysis and Gasifier Operation. Oxidative pyrolysis is a thermochemical process in which a controlled, limited amount of air is introduced into the pyrolysis reactor to partially combust the volatile gases produced during biomass decomposition. This partial combustion supplies the heat necessary to maintain the reactor temperature at approximately 600 °C, which is optimal for biochar production. Under these conditions, the oxygen in the introduced air is fully consumed within the reactor, resulting in a pyrolysis gas mixture characterized by a high content of inert gases – typically up to 50 % nitrogen (N_2) and 20 % carbon dioxide (CO_2). The remaining fraction consists of combustible gases, such as hydrogen (H_2), carbon monoxide (CO), and methane (CH_4). Due to the high proportion of ballast gases (N_2 and CO_2), the calorific value of the resulting pyrolysis gas is relatively low.

A practical application of oxidative pyrolysis for biochar production is the use of a fan-forced top-lit updraft gasifier or stoves with air supplied from below. This type of gasifier is well-suited for small-scale, distributed biochar production and serves the dual function of generating both charcoal and usable heat.

The gasifier operates under a stratified combustion–pyrolysis regime that can be divided into four key zones:

(i) a gas evolution and fuel ignition zone at the top,

(ii) a biochar layer zone,

(iii) a downward-moving gasification zone, and

(iv) an underlying unreacted biofuel layer.

The charcoal yield can be maximized by timely removal of the charred material followed by rapid quenching, which halts further oxidation and preserves the carbon-rich solid product.

Biochar production by oxidative pyrolysis was conducted using: i) a 10-liter stainless steel reactor in a household stove; ii) a 100-liter stainless steel reactor in a farmer's stove. Fig. 1 *a*, *b* show the portable household stove and the farmer's stove, respectively, according to the authors [64, 65]. Both stoves were used to process feedstock by oxidative pyrolysis, and, in the oxidative pyrolysis technology, their open-top reactors were operated with limited air access [64, 65]. To minimize environmental pollution from noxious gases, the hot pyrolysis gas released during the process was flared. The oxidative pyrolysis temperature at processing of *Miscanthus* pellets monitored by thermocouples was regulated with fan assistance controlling by the

air flow rate and the volume of air injected into the oven reactors by fans. After pyrolysis, the biochar powders were left in the reactors to cool down to room temperature and used for further analysis.

Fig. 1. (*a*) Household portable and (*b*) farmer's stoves for oxidative pyrolysis of biomass, adapted from [64, 65]

Dry pyrolysis. Dry pyrolysis experiments used to elaborate an alternative method of biochar production with the *Miscanthus* feedstock were performed in a muffle furnace (TermoLab, SNOL 8.2/1100, Ukraine) without oxygen or with minimal oxygen supply. The feedstock was placed in a 500 mL ceramic cup with a lid, filling it to 70−90 % of its total volume. Given the densities of *Miscanthus* chips (~ 150 kg/m^3) and *Miscanthus* pellets (~ 655 kg/m^3), this means that about 100 mL of air, which includes around 21 mL of oxygen, remains in the cup. This oxygen volume is significantly lower than what is required for the complete oxidation (combustion) of the loaded lignocellulosic biomass. The feedstock was then subjected to pyrolysis at constant temperatures of 400, 500, 600, or 700 °C, with a maximum residence time of 40 minutes. For dry pyrolysis, the muffle furnace was heated to a pre-set temperature at a rate of 100 °C per minute.

After pyrolysis, the cup was left in the furnace to cool to room temperature. All prepared biochar solids were weighed, and then the solids produced were ground to powders that pass through between 2.0 and 0.5 mm sieves for further standard analysis and use.

Parameters of feedstock and prepared biochars. In all pyrolysis experiments, the yield of biochar, as an indication of the weight efficiency of the pyrolysis process, was calculated as follows

$$\text{Yield } \% = (w_p/w_0)\times 100, \quad (1)$$

where w_0 is the weight of biomass before pyrolysis, and w_p is the weight of biochar. The biochar yield was 21−22 % per working weight of pellets at 10 % moisture content.

The weight fraction of volatile substances and ash were determined using the American Society for Testing and Materials (ASTM) D-5142 method [66]. Volatile substance content was determined as weight loss after heating the *Miscanthus* pellets in a covered cup to 850 °C and held for 7 min. Ash content was determined as weight loss after combustion of biochar at 750 °C in air for 6 h, in an open ceramic cup.

The weight fraction of fixed carbon was calculated by the following equation:

$$\text{Fixed carbon } \% = 100\ \% - (\text{Ash } \% + \text{Volatile substances } \% + \text{Water } \%). \quad (2)$$

Besides, the specific surface area (SSA) [67], total pore volume by water sorption [68], weight fraction of moisture [69], weight fraction of volatile substances [70, 71], weight fraction of fixed carbon [72], weight fraction of ash [73] in the prepared biochar samples were determined by the ASTM protocols.

Bulk density is obtained by dividing the dry weight of the sample by its total volume. Sulphur content was determined by Eschka method [74].

Thermal analysis. Thermogravimetric studies were performed to investigate the thermal properties of the feedstock and the produced biochar samples. Thermogravimetric data were recorded with an average weight error of 0.1 mg.

Thermogravimetric (TG), differential thermogravimetric (DTG), and differential thermal analysis (DTA) thermograms were collected using a computerized instrument Derivatograph Q-1500 D (Paulik, Paulik & Erdey, MOM, Budapest, Hungary) when samples weighing 0.1 g were heated in air at a heating rate of 10 °C min^{-1} in the temperature range from 30 to 1000 °C. The thermograms were acquired under the following mode: sensitivity – 50 mg, TG-500, DTG-500, DTA-250, leveling crucible – Al_2O_3. Melting point of ash was found from DTA thermograms.

Calorific values were determined in the static air atmosphere. The parameters of recording DTA curves were the sample weight of 50 ± 1 mg; heating from 20 to 1000 °C, heating rate of 10 °C per min. The essence of this method is to compare the area of the exothermic effect peak under the DTA curve of miscanthus biochar and that of the rhombic sulfur standard. The calorific value of sulfur is assumed to be 9.28 MJ/kg.

Fourier Transform Infrared (FTIR) spectroscopy. FTIR spectra were recorded to identify the functional groups of all biochar samples produced. The spectra, recorded with a resolution of 4 cm^{-1} in the spectral range between 4000 and 500 cm^{-1}, were collected using an FTIR spectrometer (Shimadzu IRTracer-100) operated in the attenuated total reflection (ATR) mode. At least three measurements were taken for each biochar sample using the ATR accessory at 20 °C. The biochar samples were pressed against the diamond surface using a metal rod and continuous mechanical pressure to ensure perfect contact.

RESULTS AND DISCUSSION

The research was conducted in the following phases.

Phase 1: Feasibility of biochar production from *Miscanthus* chips. We first evaluated the feasibility of producing biochar from *Miscanthus* chips 1 and 2. The initial moisture content of the both *Miscanthus* chips was approximately 43 %. Prior to using the *Miscanthus* chips, they were pre-dried to 30 % residual moisture and fed into the portable household stove reactor (Fig. 1). However, the 30 % moisture feedstock failed to ignite. In subsequent trials, the *Miscanthus* chips were further dried indoors to 9 % residual moisture, to achieve a bulk density of 140 kg/m³, which significantly improved combustion.

Phase 2: Modification of feedstock combustion conditions. To improve aeration over the reactor area, we modified the feedstock composition by introducing *Miscanthus* pellets to reach 15 % (by weight) of the *Miscanthus* chips. The technical characteristics of the *Miscanthus* pellets are shown in Table 1.

Table 1. Technical characteristics of *Miscanthus* pellets

Parameter	Indicator
Fraction (diameter), mm	8
Pellet length (max.), mm	30
Weight fraction of ash, %, by ASTM D-1506, not more than	3
Weight fraction of moisture, %, by ASTM D-1509, not more than	10
Bulk density, kg/m³	655
Calorific value, MJ/kg	17.91–19.87
Melting point of ash, °C	1185
Sulphur content (S), %, not more than	0.02
Weight fraction of volatile substances, %, by ASTM D-1620, ASTM D-5832	88

Miscanthus pellets were arranged on the grate of the oxidative pyrolysis stove, after which a layer of wood chips was placed on top and the fuel bed was ignited with a gas burner from the top. During operation, it was observed that the combustion of the pyrolysis gases occurred primarily in the vicinity of the reactor walls rather than being uniformly distributed across the entire cross-section, as would normally be expected in true oxidative pyrolysis technology. This uneven combustion behavior was mainly attributed to the flat and plate-like geometry of the chips, which blocked the interparticle spaces, restricted airflow, and directed the gas flow along the reactor walls where hydraulic resistance was lowest (Fig. 2).

Fig. 2. Visualization of chips heating and charring in the stove reactor

As a result of heat transfer from the reactor walls to the center, the chips are externally heated, like dry pyrolysis reactors. Due to the thermal resistance of the feedstock, the chips in the center of the reactor reach lower temperatures than those near the walls. As a result, the properties of the biochar, which is known from the literature [75, 76] depending on the pyrolysis temperature [77, 78], are expected to vary in different sections of the reactor.

Phase 3: Co-firing of wood chips and *Miscanthus* chips. In this phase, the feasibility of co-firing wood chips with *Miscanthus* chips in different proportions was investigated. However, during the combustion, instability and uneven burning were observed due to the formation of zones with different hydrodynamic resistances inside the reactor. The resulting biochar consisted of charred wood chips and *Miscanthus* chip ash. In our opinion, the much larger wood chips (particle size up to 10 × 20 × 25 mm) underwent gradual carbonization, while the smaller *Miscanthus* chips (0.3 × 8 × 10 mm) burned rapidly and served primarily as a heat source for pyrolysis.

The Phase 1–3 results indicate that it is inappropriate to use and process *Miscanthus* chips separately and mixed with wood chips in oxidative pyrolysis reactors to produce biochar with excellent and repeatable characteristics.

The Phase 3 results suggest that *Miscanthus* chips, whether used alone or mixed with wood chips, are not suitable for oxidative pyrolysis reactors if the goal is to produce high quality, consistent biochar. The flat shape of *Miscanthus* chips caused uneven airflow in the reactor, leading to varying temperatures across the reactor and inconsistent biochar properties. This suggests the need for better feedstock composition and reactor design for uniform combustion.

Phase 4: Comparison of oxidative and dry pyrolysis. To compare the potential of oxidative pyrolysis and dry pyrolysis, we processed *Miscanthus* pellets using the aforementioned 10- and 100-liter reactors of the specialized stoves and the muffle furnace under constant temperature conditions.

Table 2. Parameters of biochar produced from *Miscanthus* pellets by oxidative pyrolysis (No 1–2) and dry pyrolysis (No 3)

No	Biochar production units	Weight of pellets, kg	Biochar produced, kg	Biochar yield, %	Temperature, °C	Pyrolysis time, min	Average production energy demands, W/kg of biochar
1	Portable household stove	4.83	1.00	21	600	150	5.0
2	Farmer's stove	41.25	9.10	22	600	240	3.0
3	Muffle furnace	0.35	0.09	26	600	30	~10000

The key parameters of biochar production from *Miscanthus* pellets feedstock using both stove-based oxidative pyrolysis and muffle furnace dry pyrolysis are summarized in Table 2, including feedstock weight, biochar yield, pyrolysis temperature and time, and the corresponding energy demands.

From the tabulated data, it is clear that the controlling parameter in biochar production is the pyrolysis temperature, which directly affects the carbon content of the biochar. Waste wood is typically pyrolyzed at 400–500 °C [79], and the carbon content of the biochar is 65–75 %. Previously, in the case of *Miscanthus* biomass conversion to biochar, the optimal process temperature was found to be 500–600 °C, and under this condition, the carbon content in biochar is 80–90 % [80]. Therefore, the processing of miscanthus pellets by oxidative pyrolysis was carried out at the temperature of 600 °C. In the case of oxidative pyrolysis, the temperature in the stainless-steel reactors of the ovens used, monitored by thermocouples, can be regulated by the air flow rate and the volume of air injected into the oven reactors by fans. In these production units, the energy consumption for biochar production was as low as 3–5 W per kg of biochar. As can be seen from Table 2, the biochar yield in the ovens used was 21–22 % of pellet dry weight. When the pyrolysis process in the stoves was carried out in steady-state mode, the calorific value of the pyrolysis gas is 6.5 MJ/m^3.

Table 2 also shows that the use of the muffle furnace (dry pyrolysis) resulted in the highest biochar yield (26 %), while the use of the stoves (oxidative pyrolysis) resulted in slightly lower biochar yields (21–22 %). In terms of energy requirements, the muffle furnace required significantly more energy (~ 10.000 W/kg), making it much less energy efficient than either stove. Thus, the stoves had much lower energy requirements, with the "farmer" stove being the most efficient (3 W/kg biochar). In terms of pyrolysis time, the oxidative pyrolysis methods took much longer (150–240 min) than the muffle stove, which completed the pyrolysis feedstock in only 30 min. In terms of pellet processing capacity, both stoves processed a much larger amount of *Miscanthus* pellets compared to the muffle furnace. In conclusion, oxidative pyrolysis results in a slightly lower biochar yield in both stoves but is much more energy efficient and can process larger amounts of feedstock. Dry pyrolysis in the muffle furnace produces slightly more biochar, but at an extremely high energy cost, making it less practical for large-scale production.

Chips from two types of *Miscanthus* biomass, *Miscanthus* chips 1 and chips 2, and pellets from Miscanthus waste were used for further studies. The effect of pyrolysis temperature and time as process parameters on the properties of the resulting biochar was investigated. The results are shown in Table 3.

Table 3. Effect of dry pyrolysis temperature and time on the yield and SSA of the resulting biochar derived from *Miscanthus* chips 2

Pyrolysis temperature, °C	Pyrolysis time, min	Biochar yield, %	SSA, m^2/g
400	30	38	16
500	30	25	174
600	20	20	498
600	30	21	419
600	40	18	563
700	30	17	560

From Table 3, when the dry pyrolysis temperature is increased from 400 to 500 °C, the SSA of the resulting biochar increases by a factor of 10 at the same holding time of 30 min. Further increasing the pyrolysis temperature from 500 to 600 °C with the same holding time of 30 min increases the SSA of the biochar prepared by 2.4 times, while further increasing the pyrolysis temperature from 600 to 700 °C with the same holding time of 30 min increases the SSA of the resulting biochar by only 1.33 times. A similar effect of temperature in increasing the SSA of biochar has been reported previously in Ref. [81–83], considering the data for biomass waste from other crops as feedstocks. Table 3 also shows that increasing the process temperature trivially decreases the biochar yield. At 400 °C, the yield is 38 %, while at 700 °C, it drops to 17 %. This temperature trend is consistent with the typical pyrolysis process, where higher temperatures lead to increased decomposition of organic matter and greater volatilization, reducing the final biochar mass. The effect of temperature on SSA is clearly seen from Table 3. The biochar

SSA increases significantly with pyrolysis temperature. At 400 °C, the SSA value is 16 m^2/g only, but at 600 °C (20 min), it reaches 498 m^2/g, and at 700 °C (30 min), it peaks at 560 m^2/g. This increase is due to greater thermal degradation, which removes volatile compounds and creates more porosity in the biochar structure. The highest SSA (563 m^2/g) is observed at 600 °C (40 min), suggesting that both temperature and duration influence SSA development; the effect of pyrolysis time on biochar properties is seen for the most at 600 °C, varying the pyrolysis time significantly affects the SSA: 20 min: 498 m^2/g, 30 min: 419 m^2/g (decrease), and 40 min: 563 m^2/g (increase). Longer pyrolysis time generally increases SSA, but too long a time can cause structural collapse of the porous structure, which decreases SSA. Biochar yield consistently decreases with longer pyrolysis times, dropping from 21 % (30 min) to 18 % (40 min) at 600 °C; when considering optimal pyrolysis conditions, lower temperatures (~ 400–500 °C) are preferable for maximum biochar yield. For high SSA (porous biochar), 600–700 °C with optimal time (40 min at 600 °C or 30 min at 700 °C) is ideal. The choice of regime depends on the intended application. On the one hand, higher yields of biochar are better for soil amendment and carbon sequestration. On the other hand, higher SSA of biochar makes it more effective for adsorption (e.g. water filtration, contaminant removal). It can be concluded that higher pyrolysis temperatures (600–700 °C) and longer times increase porosity but decrease biochar yield. For balanced biochar production, 600 °C for 30–40 min provides a good trade-off between biochar yield and SSA. These results can guide the selection of optimal pyrolysis conditions for specific biochar applications.

The influence of *Miscanthus* feedstock type (chips or pellets) and processing method (oxidative or dry pyrolysis) on biochar properties can be further assessed from Table 4; For comparison, biochar indicators from oxidative pyrolysis of wood waste are also provided.

Table 4. Results of studies of the biochar prepared from different feedstock by oxidative and dry pyrolysis

Indicator	Biochar prepared by and originated from					
	oxidative pyrolysis			dry pyrolysis		
	Miscanthus		Wood waste	*Miscanthus*		
	Pellets	Chips 1		Pellets	Chips 1	Chips 2
Specific surface area, SSA, m^2/g, by ASTM D-6556	187	120	109	152	350	419
Total pore volume by water sorption, cm^3/g, by ASTM D-1513	0.6	3.1	1.9	0.5	2.0	2.4
Weight fraction of moisture, %, by ASTM D-1509	3.0	8.4	4.8	1.9	4.1	3.8
Weight fraction of volatile substances, %, by ASTM D-1620, ASTM D-5832	8.2	6.0	5.6	11.2	11.6	20.2
Weight fraction of fixed carbon, %, by ASTM D1762-84	82.5	80.0	85.1	77.6	76.9	72.0
Weight fraction of ash, %, by ASTM D-1506	9.3	14.0	9.3	11.2	11.5	7.8
Calorific value, MJ/kg	28.1	25.9	28.9	21.3	22.1	23.5

Table 4 shows that dry pyrolysis can produce a biochar (especially from *Miscanthus* chips 2) that has a higher SSA value of 419 m^2/g compared to that obtained by oxidative pyrolysis, SSA_{max} value of 187 m^2/g. This indicates greater porosity of biochar prepared by dry pyrolysis, making it more suitable for adsorption-based applications (e.g., pollutant removal). Biochar prepared from *Miscanthus* chips 1 by oxidative pyrolysis has the highest pore volume (3.1 cm^3), indicating improved water retention. Biochar samples prepared by dry pyrolysis of *Miscanthus* chips have lower pore volumes (max. 2.4 cm^3/g), which may affect water adsorption efficiency. Fixed carbon content is highest in the sample of wood waste biochar prepared by oxidative pyrolysis (85.1 %), followed by the biochar prepared from *Miscanthus* pellets (82.5 %). This makes biochar prepared by oxidative pyrolysis preferable for carbon sequestration and long-term soil improvement. Biochar prepared by dry pyrolysis from *Miscanthus* chips 2 has the lowest ash

content (7.8 %), while the biochar obtained from *Miscanthus* chips 1 by oxidative pyrolysis has the highest ash content (14 %). Lower ash content increases the purity of the biochar, making it more effective for industrial applications. The highest "energy harvesting" is observed in biochar produced from wood waste with the highest calorific value of 28.9 MJ/kg, followed by biochar from *Miscanthus* pellets produced by oxidative pyrolysis (28.1 MJ/kg). Dry pyrolysis biochar has lower calorific values (21.3–23.5 MJ/kg), making it less suitable to be applied as solid fuel. In conclusion, for adsorption applications (water filtration, pollutant removal), biochar obtained by dry pyrolysis from *Miscanthus* chips 2 is preferred due to its high SSA and porosity. For soil improvement and carbon sequestration, biochar prepared by oxidative pyrolysis of *Miscanthus* pellets and wood waste is ideal due to its higher fixed carbon content. In addition, for applications as solid fuel, wood waste biochar prepared by oxidative pyrolysis is optimal due to its advanced calorific value.

As shown in Fig. 3, the combustion characteristics of the *Miscanthus* chips 1 sample were evaluated using TG-DTG analysis. Here, the thermograms show areas of thermal destruction with removal of volatile samples and thermolysis of "fixed" carbon in the temperature intervals of 200–380 and 380–500 °C, respectively [84–88]. According to the DTG results, dehydration of the sample from physically adsorbed water occurs at 50–140 °C, with a maximum at about 95–101 °C (endothermic effect). Hemicellulose thermal degradation occurs in the range of 230–360 °C, with a maximum of about 291–296 °C. Cellulose thermal degradation occurs in the range of 285–380 °C with a maximum at 334–335 °C. Thermal destruction of lignin, on the other hand, is slow and occurs in the range of 200–700 °C, with a maximum at 381 °C. When heated, *Miscanthus* chips are capable of thermal spontaneous combustion; smoldering temperature and spontaneous combustion temperature at 204 and 333 °C, respectively.

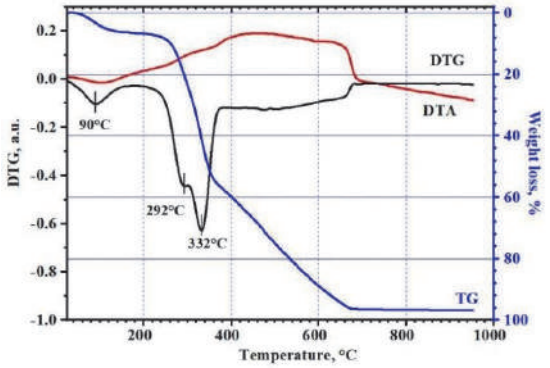

Fig. 3. TGA-DTA of the *Miscanthus* chips 1

The DTA curve in Fig. 3 indicates the presence of a narrow endothermic effect in the range of 50–140 °C and a wide exothermic effect in the range of 140–690 °C, as well as the processes of drying pyrolysis, thermal destruction and combustion under the influence of high temperatures and oxygen during heating. In the process of thermal studies, it is possible to distinguish stages realized in different temperature intervals.

Studies of the thermal properties of *Miscanthus*-derived biochar have shown that for the first endothermic effect, the maximum dehydration temperatures are slightly lower than those for *Miscanthus* raw materials, and the mass losses are comparable (Fig. 4 *a*). Lower maximum temperatures of the effect indicate a higher content of physisorbed water [89]. The pellet biochar is characterized by the highest weight loss of 10 %. The second (exothermic) effect of weight loss due to thermolysis, oxidation, and off-gassing of volatile substances [90] is observed in a wide temperature range with a blurred and not clearly defined maximum. However, for all biochar samples studied (Fig. 4 *b*), the onset of the effect is observed at a temperature close to 272 °C, and the end of the effect is observed at 737 °C. In the case of charcoal, there is an additional intense weight loss effect that is superimposed on the above exothermic effect. This peak and the corresponding weight loss effect

may correspond to a more intense concomitant oxidative thermolysis process. According to DTG data (Fig. 4 *c*), this process is characterized by a maximum at 364 °C and a weight loss of 8 %. It should be noted that the highest weight loss in the second process of 16 % characterizes biochar from chips 2. Based on the DTA data, it is likely that the complex weight loss effect has at least three components, which can be characterized by maxima at 241, 377–419, and 650 °C. The second exothermic high temperature weight loss effect is observed on the DTG curves in the temperature range of 806–817 °C, but the maximum of the process for charcoal is shifted to higher temperatures up to 831 °C.

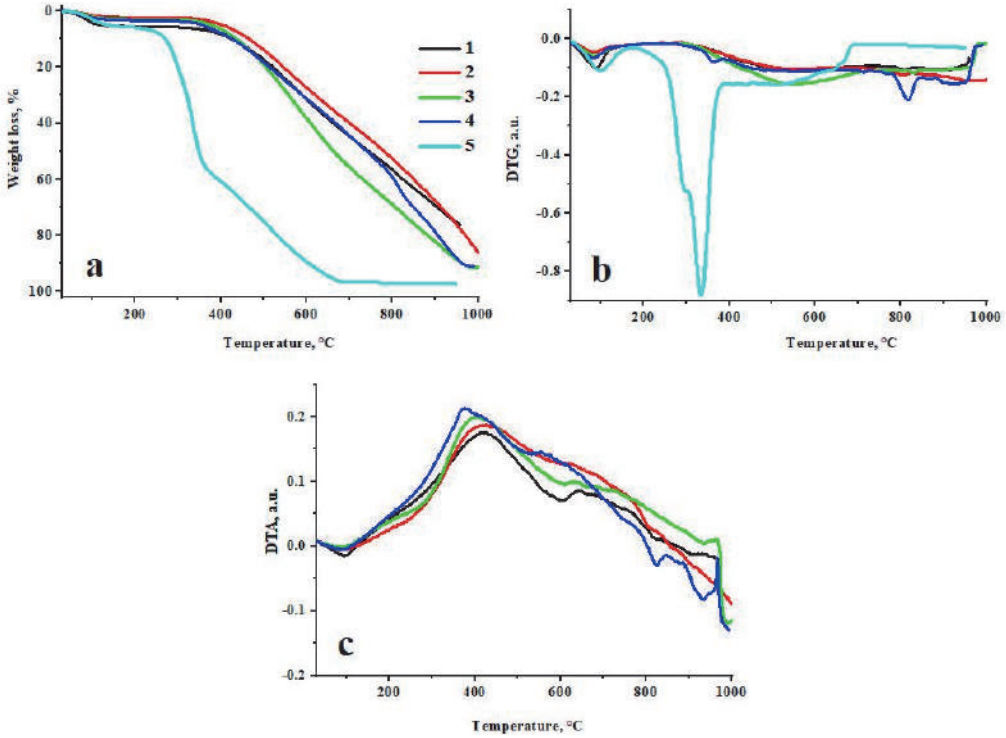

Fig. 4. (*a*) TG, (*b*) DTG, and (*c*) DTA of biochars: *1* – biochar from *Miscanthus* pellets, *2* – biochar from *Miscanthus* chips 1, *3* – biochar from *Miscanthus* chips 2, *4* – charcoal, *5* – *Miscanthus* chips 1

Table 5. Thermal characteristics of biochar

Sample	Temperature at the effect maximum, °C	Weight loss, %
Endothermic effect maximum in the temperature range 40–136 °C		
Biochar from *Miscanthus* pellets	88	10
Biochar from *Miscanthus* chips 1	85	5
Biochar from *Miscanthus* chips 2	87	6
Charcoal from wood waste	83	7
Exothermic effect maximum in the temperature range 272–740 °C		
Biochar from *Miscanthus* pellets	562	11
Biochar from *Miscanthus* chips 1	548	10
Biochar from *Miscanthus* chips 2	544	16
Charcoal	541	11
Exothermic effect maximum in the temperature range 771–858 °C		
Biochar from *Miscanthus* pellets	807	11
Biochar from *Miscanthus* chips 1	806	13
Biochar from *Miscanthus* chips 2	831	12
Charcoal from wood waste	817	21

Within the temperature range of 806–817 °C, charcoal is characterized by the highest weight loss of 21 % among the samples studied, while *Miscanthus* biochar samples lose no more than 13 % of the sample weight (Table 5). The highest temperature effect of weight loss with a maximum at 912 °C for biochar samples from pellets and *Miscanthus* chips 2 is characterized by a weight loss of 10 %, it is likely that this effect on the DTG curves for charcoal is shifted to high temperatures up to 926 °C (weight loss of 16 %), and for the *Miscanthus* chips 1 sample it is observed at 985 °C (weight loss of 14 %). As a result of the thermogravimetric study, charcoal loses 91.7 % and *Miscanthus* biochar loses 86.2–92 % of the total sample weight. The highest ash content is observed for the sample of biochar from miscanthus pellets at 3.8 % level.

Therefore, the TG and DTG curves (Fig. 4 *a*, *b*) were analyzed for thermal stability. The analysis was done to determine the peculiarities of pyrolysis and oxidation of biochar obtained at different process temperatures. According to the DTG curves (Fig. 4 *b*), considering the temperatures at which the maximums are observed, the number of thermal peaks and their shapes can differ significantly for different samples of biochar and charcoal, which may indicate their structural differences. The initial thermal peaks, which were recorded at temperatures ranging from 83 to 88 °C, were attributed to the weight loss of moisture during the dehydration process. Notably, the biochar sample prepared from *Miscanthus* pellets exhibited the highest moisture content, while the moisture content of the two biochars prepared from miscanthus chips was comparable. The DTA curves (Fig. 4 *c*) demonstrate that the existing components contribute to the total exothermic effect within the temperature range of 200–400 °C. The presence of these components is likely associated with the weight loss related to hemicellulose and cellulose remaining after the thermal processing of raw materials. It is noteworthy that the remaining components with substantial contribution to the observed temperature-extended effect anticipated within the temperature range of 370–550 °C, are associated with the thermal decomposition of lignin. The weight loss and the corresponding effects manifested by the presence of sharp peaks on the DTG curves (Fig. 4 *b*) in the temperature range of 300–480 °C may be the result of the auto-catalytic reaction of hemicellulosic, cellulosic, and lignocellulosic components of the obtained biochar [91]. As the temperature of pyrolysis and oxidation by air oxygen increases, the number of peaks in the thermograms decreases, and the appearance of new temperature-extended effects correspond to a combination of thermolysis and oxidation reactions. Consequently, DTA registers a spectrum of exothermic processes, the course of which is shifted towards high temperatures relative to those of the feedstock. The course of thermolysis and combustion at higher temperatures indicates the removal of the usual hemicellulosic and cellulosic derivatives and the formation of more thermostable related substances because of the heat treatment used to obtain biochar from *Miscanthus*.

Fig. 5 *a–c* shows a photograph of the biochar produced under optimal conditions. The texture changes from fine flakes (Fig. 5 *a*) to small granules (Fig. 5 *b*) to solid large pellet-like forms (Fig. 5 *c*). Fig. 5 *a* shows fine black flakes that appear irregular in shape and size, up to 0.5 cm long; Fig. 5 *b* shows slightly larger black granules that are coarser and more irregular than the left section. Fig. 5 *c* shows cylindrical black granules, some of which are broken into smaller fragments. The largest pieces in the Fig. 5 *c* are about 1–2 cm long. Some black dust is visible around the pellets, especially in Fig. 5 *b* and Fig. 5 *c*.

The FTIR ATR spectra of *Miscanthus*-derived biochar (Fig. 6) can be interpreted in two principal regions containing characteristic bands associated with carbonyl, hydroxyl, and aliphatic C–H groups. It should be kept in mind that biochar spectra are inherently complicated due to overlapping signals from thermally degraded cellulose, hemicellulose, lignin, and inorganic residues. Additionally, peak positions and intensities may shift slightly depending on pyrolysis temperature and elemental composition. The spectral data were analyzed using LabCognition's irAnalyze-RAMalyze software (www.labcognition.com) and validated with relevant literature sources [92–94].

The FTIR-ATR spectra revealed a range of characteristic absorption bands associated with various oxygen-containing functional groups.

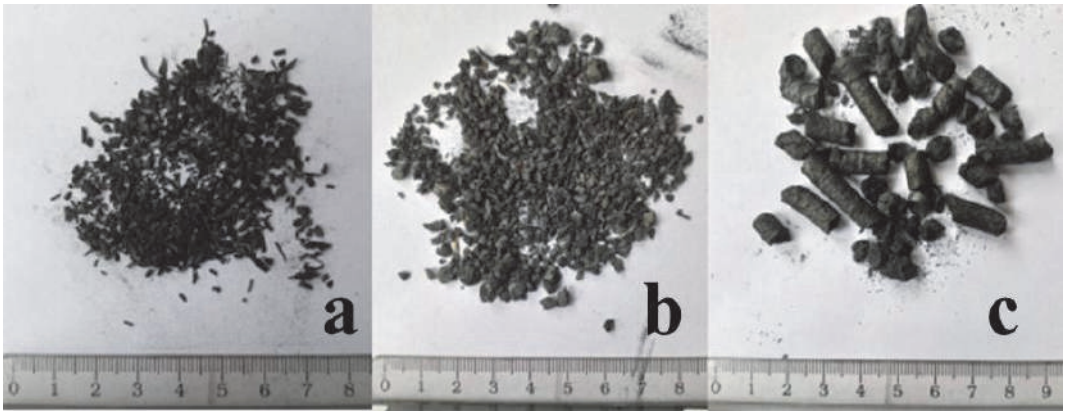

Fig. 5. Photos of biochar from *Miscanthus* chips 1 (*a*) and 2 (*b*), and biochar from *Miscanthus* pellets (*c*), all the biochar solids were prepared under the optimal dry pyrolysis conditions

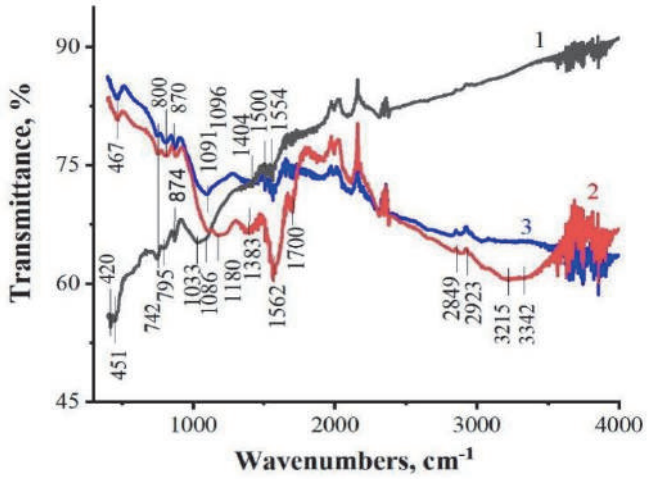

Fig. 6. FTIR ATR spectra of biochars obtained from: *1 – Miscanthus* chips 1, *2 – Miscanthus* chips 2, *3 – Miscanthus* pellets prepared under the optimal conditions

In the low-frequency region, bands observed at 420, 450, and 467 cm^{-1} are attributed to carbonate bending vibrations (C–O) and lattice vibrations involving metal–oxygen or silicon–oxygen bonds, likely arising from mineral residues in the feedstock. Peaks at 742, 795, and 800 cm^{-1} correspond to out-of-plane bending vibrations of aromatic C–H bonds, typical of substituted aromatic structures, and became more pronounced in the biochar spectra. Absorption bands at 870 and 874 cm^{-1} suggest the presence of cyclic acid anhydride groups (C–C and C–O), as well as aromatic C–H bending. Prominent bands at 1033, 1086, and 1091 (1096) cm^{-1} are associated with asymmetric stretching of Si–O–Si or Si–O–C bonds, and may also reflect C–O stretching from residual polysaccharides. The presence of large, complex carbohydrates may explain the higher moisture uptake observed in biochar derived from chips 2 (spectrum 2) compared to other samples, as carbohydrates are hydrophilic due to their saturation with hydroxyl groups. Peaks at 1383 and 1404 cm^{-1} are attributed to symmetric stretching of carboxylate groups (COO^-) and bending vibrations of methyl (CH_3) groups. Bands at 1500, 1554, and 1562 cm^{-1} are consistent with aromatic C=C skeletal vibrations and may also reflect N–H bending from nitrogenous compounds. The absorption at 1700 cm^{-1} is associated with carbonyl (C=O) stretching vibrations, arising from ketones, aldehydes, or conjugated carboxylic groups. It may also reflect the presence of aromatic aldehydes (Ar–CH=O). In the higher wavenumber region, peaks at 2849 and 2923 cm^{-1} correspond to symmetric and asymmetric

stretching vibrations of aliphatic CH_2 and CH_3 groups, likely from residual lignin or waxy compounds. Broad absorption bands centered at 3215 and 3342 cm^{-1} are assigned to O–H stretching vibrations of hydroxyl groups involved in hydrogen bonding, contributing to the biochar's surface hydrophilicity. The spectral region between 1708 and 1594 cm^{-1} can be attributed to C=O stretching vibrations, commonly associated with carbonyl and carboxyl functional groups, and/or to C=C stretching from conjugated systems. Absorption bands in the 1000–1240 cm^{-1} range are typically linked to C–O stretching vibrations and, in some cases, C–S bonds–characteristic of thermal degradation products from cellulose and hemicellulose. The peak at 1404 cm^{-1} is associated with C–H deformation vibrations, commonly found in lignin and carbohydrate structures. Additionally, the region from 1270 to 1210 cm^{-1} indicates C–O stretching, consistent with lignin and xylan (a major hemicellulose component). Among these, the consistently observed peak at 1033 cm^{-1} is clearly attributed to C–O stretching in carboxylic acids, esters, and ethers–derivatives of cellulose and hemicellulose degradation–prominently featured in the biochar spectra. The peaks at 1383 and 1404 cm^{-1} are commonly observed in biomass and biochar spectra. These may be associated with C–H bending, C–C stretching, and C–O stretching vibrations in cellulose, hemicellulose, and lignin or their degradation products. Such peaks often reflect hemicellulose-derived structures before complete thermal degradation. However, assigning these bands to specific functional groups should be done cautiously, as they often overlap and are not exclusive. The peak at 1404 cm^{-1} is typically associated with O–H bending, C–H deformation, or COO^- symmetric stretching–potentially from carboxylic acids or esters beyond hemicellulose origin. Similarly, the 1383 cm^{-1} peak is often attributed to C–H bending in CH_3 groups, which may also originate from lignin or cellulose derivatives. The 1033 cm^{-1} peak, a key spectral feature, is commonly assigned to C–O stretching vibrations typical of alcohols, ethers, and polysaccharide structures. The broader region from 1000 to 1200 cm^{-1} is generally linked to C–O and C–C stretching, and, depending on composition, may also include P–O or Si–O vibrations. In the context of biochar, strong absorption in this region–especially the pronounced 1033 cm^{-1} peak–indicates the presence of oxygenated functional groups likely originating from structural residues or thermal decomposition of cellulose and hemicellulose.

Fig. 6 compares the FTIR-ATR spectra of biochar obtained from *Miscanthus* pellets and chips. While general similarities are observed, they do not necessarily reflect identical structural or chemical properties. A closer examination reveals notable differences, particularly in the 1750–1000 cm^{-1} region, which contains several diagnostically important absorption bands. Peaks within this region, especially those related to C=O stretching vibrations (typically around 1650–1750 cm^{-1}), suggest the presence of oxygen-containing functional groups and reflect structural differences arising from variations in feedstock type and pyrolysis behavior. Biochar derived from *Miscanthus* feedstock exhibits both hydrophilic and hydrophobic surface properties. Its hydrophobic character is primarily attributed to the presence of functional groups such as cyclic acid anhydrides (C–C and C–O), asymmetric carboxylates (CO_2), surface ketones (C=O), aromatic structures (C=C), silicon-containing groups (Si–O), and hydrophilic carbonates (C–O). FTIR-ATR spectroscopy revealed peaks at 3215 and 3342 cm^{-1}, corresponding to hydroxyl (–OH) groups; these peaks were least intense in spectra 1 and 3 (Fig. 6). The broad and intense band at 3342 cm^{-1} is indicative of O–H stretching vibrations. As an active bonding group, hydroxyls are commonly involved in both intra- and intermolecular hydrogen bonding. These interactions significantly influence the cohesive forces and structural integrity of biochar particles during formation. Furthermore, distinct peaks at ~ 2923 and ~ 2849 cm^{-1} correspond to asymmetric and symmetric stretching vibrations of methylene (CH_2) groups, respectively. These bands indicate the presence of hydrophobic aliphatic chains within the biochar. Their intensity, which relates to the hydrophobicity index of soil organic matter, can affect surface chemistry and interparticle interactions. Notably, spectrum 1 – representing biochar derived from *Miscanthus* chips 1 – shows a lower relative intensity at these positions, suggesting reduced hydrophobic CH_2 group content. Additionally, the peak near 1700 cm^{-1} in spectrum 2 – assigned to carboxyl C=O stretching, likely from acetyl groups formed during hemicellulose degradation – exhibits a marked decrease in

spectra 2 and 3. This decline further supports the occurrence of structural transformations during pyrolysis, which may influence the chemical reactivity and functional group composition of the resulting biochar.

Nevertheless, based on the different spectral peaks and their associated functional groups, it can be hypothesized that both the *Miscanthus*-derived biochar chips and pellet samples contain higher proportions of the groups identified above. The prepared biochar samples are characterized by oxygen-containing functional groups, which can be interpreted to mean the production of good quality granules in terms of hardness, since strong electrostatic attraction results from the presence of polar functional groups such as the oxygen-containing functional groups. In terms of energy production, this means that *Miscanthus*-derived biochar granules generally contain a variety of polar and non-polar functional groups that can facilitate the balance of the chain reactions that occur under combustion conditions. At the same time, it is important to note that biochar produced from *Miscanthus* biomass has a complicated structural composition. This structural complexity makes it difficult to understand the relationship between biomass molecular structure and energy production under thermal conditions, which requires further research.

Cellulose, hemicellulose, and lignin decompose more completely and at lower temperatures under wet pyrolysis conditions [95, 96]. However, hydrothermal carbonization produces hydrochar that typically contains lower carbon and ash contents compared to biochar. Hydrochar also exhibits lower SSA and porosity, and often contains potentially harmful byproducts such as phenolic compounds [97]. These physical limitations and chemical residues reduce its effectiveness in soil amelioration applications [98]. The differences in product characteristics are primarily attributed to variations in carbon-to-hydrogen (C/H) and oxygen-to-carbon (O/C) ratios between wet and dry pyrolysis processes [95, 96]. To fully harness the benefits of biochar, particularly for soil improvement, achieving a high SSA remains a key objective.

Typically, the SSA value of biochar plays a pivotal role in determining its effectiveness in various applications, such as soil amendment, water filtration, and carbon sequestration. According to the International Biochar Initiative (https://biochar-international.org/), biochar with a SSA value of 150 m^2 per g and above is considered of high quality, suitable for agricultural and environmental applications. In this study, biochar samples produced from *Miscanthus* pellets by oxidative pyrolysis and the charcoal sample prepared by dry pyrolysis of wood chips met this requirement, as their SSA values exceeded 150 m^2 per g. However, charcoal obtained from wood waste and biochar derived from *Miscanthus* chips 1 exhibited significantly lower SSAs, making it less effective for many applications, such as pollutant adsorption or improving soil fertility. Considering the impact of pyrolysis conditions on biochar characteristics, it is clear that pyrolysis temperature and duration play an important role in the development of SSA and other impacting properties of the resulting biochar samples. Higher pyrolysis temperatures generally result in the production of biochar with greater fixed carbon content and higher SSA values, but with a lower overall yield due to the decomposition of volatiles.

This trend is clearly observed in our results, where the biochar yield decreased significantly at higher temperatures (600 °C), but the SSA increased. The SSA of biochar is primarily determined by the formation of microporous and mesoporous structures during pyrolysis, which is enhanced at higher temperatures. Moreover, the oxidative pyrolysis used for *Miscanthus* pellets in this study may have contributed not only to a higher specific surface area, but by promoting the formation of functional groups on the biochar surface, such as hydroxyl and carboxyl groups, which can enhance the surface reactivity and total adsorption capacity. However, the presence of high ash content in biochar from a certain feedstock, particularly wood chips, can impede the development of SSA, as inorganic ash can block the pores during the pyrolysis process.

The findings from this study suggest that *Miscanthus* × *giganteus* could be a superior feedstock for producing high-surface-area biochar compared to other biomass types, especially when compared to wood chips. *Miscanthus*, being a grassy biomass, has a higher lignocellulose content and a more open cellular structure compared to wood, making it potentially more suitable for biochar production under oxidative pyrolysis conditions. In contrast, wood-derived biochar often exhibits lower SSA due to the higher lignin content, which, when pyrolyzed, tends to create a denser carbon structure that may

not promote the formation of porous structure as effectively as grassy biomass. Typically, biochar with a higher SSA is generally more effective for carbon sequestration, as it provides a greater SSA for adsorption of CO_2 and other gases. Furthermore, biochar with a higher SSA is often more effective in soil improvement, where it enhances nutrient and water retention, and pollutant adsorption, which is crucial for environmental cleanup.

Our results indicate that biochar from *Miscanthus* chips could be more beneficial for applications that require high adsorption capacities, such as water filtration or soil remediation, compared to biochar from *Miscanthus* pellets or wood chips. However, the lower yield associated with high-temperature pyrolysis conditions must be considered when scaling up production for industrial applications, as it may result in higher production costs.

Further studies are needed to investigate the long-term stability and environmental impact of biochar produced from different feedstock under varying pyrolysis conditions. In particular, research on the effect of biochar on soil microbial communities and its ability to sequester carbon over extended periods would provide valuable insights into the sustainability and environmental benefits of biochar. Additionally, a more detailed examination of biochar pore size distribution, along with adsorption tests, would help clarify the potential of *Miscanthus*-derived biochar for specific applications, such as pollutant removal or agricultural enhancement [99, 100].

CONCLUSION

The properties of biochar produced from *Miscanthus* chips and pellets by oxidative pyrolysis in stainless-steel reactors of specially constructed ovens have been investigated. The SSA of biochar from chips is 120 m^2/g, which is lower than the recommended value of 150 m^2/g. Therefore, it is advisable to process *Miscanthus* chips by dry pyrolysis. The SSA of biochar produced from *Miscanthus* pellets is 187 m^2/g, which meets the established requirements. The production of biochar from *Miscanthus* pellets in the auto-thermal oxidative pyrolysis regime requires minimal power consumption per unit of product (3...5 W/kg). It is advisable to install such reactors at pellet manufacturing plants and sell the products in the form of a biochar, which has a higher added value. The pyrolysis gas produced during biochar production should be considered as a secondary processing product. It has an average calorific value of 6.5 MJ/m^3 and can be used to produce thermal energy or electricity. Thermogravimetric studies of the produced biochar were performed, and the results can be used to develop industrial oxidative pyrolysis reactors. A further task should be to test biochar obtained from different feedstocks of *Miscanthus* × *giganteus* waste and at different pyrolysis parameters as soil amendments using standard agricultural crops, spinach or maize.

ACKNOWLEDGEMENT

The research is supported by NATO SPS MYP G6094.

Вплив вихідного стану біомаси та умов піролізу на властивості біовугілля, отриманого з відходів *Miscanthus* × *giganteus*

В.В. Підліснюк, Т.Р. Стефановська, Л.І. Борисенко, В.П. Клюс, Г.О. Четверик, А.І. Медков, В.В. Лісняк

Кафедра хімії і технології навколишнього середовища, факультет екології
Університет Яна Євангеліста Пуркіне
Пастерова, 15, 400 96, Усті-над-Лабем, Чеська Республіка
Кафедра ентомології, факультет захисту рослин, біотехнологій та екології
Національний університет біоресурсів і природокористування
вул. Героїв Оборони, 15, Київ, 03041, Україна
Інститут хімії поверхні ім. О.О. Чуйка Національної академії наук України
вул. Олега Мудрака, 17, Київ, 03164, Україна, lisnyak@nas.gov.ua
Інститут відновлюваної енергетики Національної академії наук України
вул. Гната Хоткевича, 20-а, Київ, 02094, Україна
Відділ агробіоресурсів та екологічно безпечних технологій
Інститут агроекології і природокористування
вул. Метрологічна, 12, Київ, 03143, Україна

Досліджено вплив умов піролізу та початкового стану біомаси Miscanthus × giganteus на властивості біовугілля як кінцевого продукту окиснювального та сухого піролізу. Як сировину використовували тріску та гранули з біомаси Міскантусу, а також деревні відходи. Тріска з Міскантусу була отримана з біомаси, вирощеної на сільськогосподарських або малопродуктивних ґрунтах. Вищезгадану сировину переробляли на біовугілля шляхом окиснювального піролізу в спеціально розроблених «побутових» та «фермерських» печах, а також шляхом сухого піролізу в муфельній печі. Вищі температури піролізу (600–700 °C) привели до отримання біовугілля з вищою питомою поверхнею (ПП), але з нижчим виходом. Баланс між виходом і ПП був знайдений при температурі 600 °C та часі піролізу 30–40 хвилин, що робить ці умови ідеальними для отримання високопоруватого біовугілля, придатного для адсорбційних застосувань. Для поліпшення якості ґрунту слід надати перевагу біовугіллю з пелет Міскантусу та деревних відходів завдяки вищому вмісту фіксованого вуглецю. Для адсорбційних застосувань краще використовувати сухе піролізне біовугілля з тріски Міскантусу, оскільки воно має вищу ПП. Для застосувань як палива ідеально придатне біовугілля, отримане в результаті окиснювального піролізу деревних відходів та гранул з біомаси Міскантусу, завдяки найвищій теплотворній здатності. Термогравіметричний аналіз тріски Міскантусу, нагрітої на повітрі, показав наявність процесу, що включає реакції дегідратації, піролізу та окиснення, і виявив його стадії, а саме: дегідратацію при 50–140 °C, деградацію геміцелюлози при 230–360 °C, деградацію целюлози при 285–380 °C та повільну деструкцію лігніну при 200–700 °C. Тріска з Міскантусу демонструє характерне самозайманння, тління починається при 204 °C, а повне згоряння – при 333 °C. Біовугілля, вироблене з Міскантусу, як сировини, має нижчу температуру дегідратації, ніж вихідна сировина Міскантусу, і втрачає 86.2–92 % своєї ваги під час термічної обробки. Біовугілля, отримане з гранул Міскантусу, має найвищий вміст вологи, в той час як біовугілля з тріски Міскантусу є менш гідрофільним. Термічна стабільність варіюється між зразками біовугілля, зі значними відмінностями в режимах втрати ваги під час піролізу та окиснення. Ці відмінності вказують на структурні варіації, ймовірно, пов'язані зі складом сировини та умовами піролізу. Приготоване біовугілля має як гідрофобні, так і гідрофільні властивості, що підтверджується наявністю характерних піків гідрофобних та гідрофільних груп у інфрачервоних (ІЧ) спектрах з перетворенням Фур'є. Зокрема, ІЧ-Фур'є спектроскопія вказує на наявність гідроксильних (–OH), карбонільних (C=O), карбоксильних (–COOH) та метиленових (CH_2) груп у продуктах карбонізації, отриманих зі структурних компонентів біомаси – целюлози, геміцелюлози та лігніну. Встановлено, що значення ПП біовугілля, отриманого з гранул Міскантусу окиснювальним піролізом та ПП біовугілля, отриманого сухим піролізом з тріски Міскантусу, відповідають параметрам, рекомендованим Міжнародною ініціативою з біовугілля, і становлять відповідно187 та 419 $м^2/г$. Зроблено висновок, що виробництво біовугілля з гранул Міскантусу методом окиснювального піролізу вимагає мінімальних витрат енергії на одиницю продукту. Переробка відходів Міскантусу шляхом їхнього перетворення на біовугілля є перспективним рішенням в рамках концепції циркулярної економіки, оскільки біовугілля, отримане з Miscanthus × giganteus, може бути ефективною добавкою, застосування якої сприятиме відновленню деградованих ґрунтів шляхом фіторемедіації.

***Ключові слова**: Тріска та пелети з Міскантусу, окиснювальний піроліз, сухий піроліз, температура обробки, питома поверхня біовугілля*

REFERENCES

1. Alavi-Borazjani S.A., Capela I., Tarelho L.A.C. Valorization of biomass ash in biogas technology: Opportunities and challenges. *Energy Rep*. 2020. **6**(1): 472.
2. Manyà J.J. Pyrolysis for biochar purposes: a review to establish current knowledge gaps and research needs. *Environ. Sci. Technol*. 2012. **46**(15): 7939.
3. Lee J., Sarmah A.K., Kwon E.E. Production and Formation of Biochar. In: *Biochar from Biomass and Waste: Fundamentals and Applications*. (Amsterdam: Elsevier, 2019).
4. Gui X., Xu X., Zhang Z., Hu L., Huang W., Zhao L., Cao X. Biochar-amended soil can further sorb atmospheric CO_2 for more carbon sequestration. *Commun. Earth Environ*. 2025. **6**: 5.
5. Enaime G., Lübken M. Agricultural Waste-Based Biochar for Agronomic Applications. *Appl. Sci.* 2021. **11**(19): 8914.
6. Liu Q., Zhang Y., Liu B., Amonette J.E., Lin Z., Liu G., Ambus P., Xie Z. How does biochar influence soil N cycle? A meta-analysis. *Plant and Soil.* 2018. **426**: 211.
7. Tomczyk A., Sokolowska Z., Boguta P. Biochar physicochemical properties: pyrolysis temperature and feedstock kind effects. *Rev. Environ. Sci. Biotechnol*. 2020. **19**: 191.
8. Solokha M., Demyanyuk O., Symochko L., Mazur S., Vynokurova N., Sementsova K., Mariychuk R. Soil Degradation and Contamination Due to Armed Conflict in Ukraine. *Land*. 2024. **13**(10): 1614.
9. Bonchkovskyi O., Ostapenko P., Bonchkovskyi A., Shvaiko V. War-induced soil disturbances in north-eastern Ukraine (Kharkiv region): Physical disturbances, soil contamination and land use change. *Sci. Total Environ*. 2025. **964**: 178594.
10. Pidlisnyuk V., Erickson L., Stefanovska T., Popelka J., Hettiarachchi G., Davis L., Trogl J. Potential phytomanagement of military polluted sites and biomass production using biofuel crop Miscanthus × giganteus. *Environ. Pollut*. 2019. **249**: 330.
11. Pidlisnyuk V., Newto R.A., Mamirova A. Miskanthus biochar value chain - A review. *J. Environ. Manage.* 2021. **290**: 112611.
12. Donia E., Mineo A.M., Sgroi F. A methodological approach for assessing business investments in renewable resources from a circular economy perspective. *Land Use Policy*. 2018. **76**: 823.
13. Braghiroli F.L., Passarini L. Valorization of Biomass Residues from Forest Operations and Wood Manufacturing Presents a Wide Range of Sustainable and Innovative Possibilities. *Curr. For. Rep*. 2020. **6**: 172.
14. Bożym M., Gendek A., Siemiątkowski G., Aniszewska M., Malaťák J. Assessment of the Composition of Forest Waste in Terms of Its Further Use. *Materials*. 2021. **14**(4): 973.
15. Biohar Market (Forecast, 2021-2031), 2021. https://www.transparencymarketresearch.com/biochar-market.html
16. Kramar V., Kramar V. Economic efficiency of the production of biochar and solid fuel based on biocal. *Thermophys. Therm. Power Eng.* 2024. **46**(2): 110.
17. Yaashikaa P.R., Kumar P.S., Varjani S., Saravanan A. A critical review on the biochar production techniques, characterization, stability and applications for circular bioeconomy. *Biotechnol. Rep*. 2020. **28**: e00570.
18. Kwapinski W., Byrne C.M.P., Kryachko E., Wolfram P., Adley C., Leahy J.J., Novotny E.H., Hayes M.H.B. Biochar from biomass and waste. *Waste Biomass Valori*. 2010. **1**(2): 177.
19. Amalina F., Abd Razak A.S., Krishnan S., Sulaiman H., Zularisam A.W., Nasrullah M. Biochar production techniques utilizing biomass waste-derived materials and environmental applications – A review. *J. Hazard. Mater. Adv*. 2022. **7**: 100134.
20. Libra J.A., Ro K.S., Kammann C., Funke A., Berge N.D., Neubauer Y., Titirici M.-M., Fühner C., Bens O., Kern J., Emmerich K.-H. Hydrothermal carbonization of biomass residuals: a comparative review of the chemistry, processes and applications of wet and dry pyrolysis. *Biofuels*. 2011. **2**(1): 71.
21. Bugge G. *Industrie der Holzdestillations-Produkte*. (Dresden and Leipzig, Germany: Theodor Steinkopff, 1927).
22. Gubinsky M.V., Shishko Yu.V., Shevchenko G.L., Usenko A.Yu., Fedorov S.S., Kremneva K.V. Research of the process of pyrolysis of biomass waste in a dense layer. *Integr. Technol. Energy Conserv*. 2008. **2**: 29.
23. Karp I.N., Martsevoy E.P., Pyanykh K.E., Antoshchuk T.A., Pyanykh K.K. Research and implementation of coal and biomass gasification processes to replace natural gas. *Energy Technol. Resour. Sav.* 2014. **4**: 3.
24. Klyus S.V., Zhovmir M.M., Maslyukova Z.V., Demchina V.P. Evaluation of main parameters and efficiency of partial biomass gasification in fixed bed gasifier with inverse blowing. *Vidnovliuvana energetyka*. 2016. **2**: 79.
25. State Standard of Ukraine. (DSTU 7502:2014)
26. Nowak A. *Chemische Holzverwertung*. (Vienna, Austria: Hartleben, 1932).
27. Tokay B.A. Biomass Chemicals. In: *Ullmann's Encyclopedia of Industrial Chemistry*. (Weinheim: Wiley-VCH, 2005).
28. Bridgwater A.V. Pyrolysis – state of the art. In: *Success & Visions for Bioenergy: Thermal Processing of Biomass for Bioenergy, Biofuels and Bioproducts*. Bridgwater A.V. (editor). (Newbury, Berks, UK: CPL Press, 2007).

29. Antal M.J., Gronli M. The art, science, and technology of charcoal production. *Ind*. *Eng*. *Chem*. *Res*. 2003. **42**(8): 1619.
30. Laughton M.A. (editor). Biofuels. In: *Renewable Energy Sources: Watt Committee:* Report Number 22. (London: Taylor & Francis, 2004).
31. Lewandowski M., Milchert E. Modern technology of dry distillation of wood. *CHEMIK*. 2011. **65**(12): 1301.
32. Gautam R., Mittal V., Chauhan A., Jaiswal A., Ghosh U.K. Biochar-Derived Green Catalysts for Biofuel Production. In: *Encyclopedia of Green Materials*. Baskar C., Ramakrishna S., Rosa A.D.L. (editors). (Singapore: Springer, 2025).
33. Kandiyoti R., Herod A., Bartle K.D., Morgan T.J. *Solid Fuels and Heavy Hydrocarbon Liquids: Thermal Characterization and Analysis*. (Amsterdam: Elsevier, 2016).
34. Farooq S., Fatima, Aziz H., Riaz U., Rizwan M. Soil Health Improvement and Pollution Remediation Using Biochar. In: Kiran (editor) *Biochar Revolution. Sustainable Landscape Planning and Natural Resources Management.* (Cham: Springer Nature, 2025).
35. Ok Y.S., Uchimiya S.M., Chang S.X., Bolan N. (Editors). *Biochar: Production, characterization, and applications*. (Boca Raton: CRC Press, 2015).
36. Bergna D., Romar H., Tuomikoski S., Runtti H., Kangas T., Tynjälä P., Lassi U. Activated Carbon from Renewable Sources: Thermochemical Conversion and Activation of Biomass and Carbon Residues from Biomass Gasification. In: *Waste Biomass Management – A Holistic Approach.* Singh L., Kalia V.C. (editors). (Cham: Springer, 2017).
37. Liu H., Basar I.A., Nzihou A., Eskicioglu C. Hydrochar derived from municipal sludge through hydrothermal processing: A critical review on its formation, characterization, and valorization. *Water Res*. 2021. **199**: 117186.
38. Mašek O. Biochar Preparation by Different Thermo-Chemical Conversion Processes. In: Méndez A., Mohan D., Masek O., Ramola S., Tsubota T. (Editores). *Engineered Biochar: Fundamentals, Preparation, Characterization and Applications*. (Singapore: Nature Springer, 2022).
39. Cavalloni F.C., Strassburg J., Lustenberger D., Griffin T. Oxidative Pyrolysis for Variable Heating Output with Wood Pellets. *Energies*. 2025. **18**(7): 1702.
40. Huang Y., Li B., Liu D., Xie X., Zhang H., Sun H., Hu X., Zhang S. Fundamental Advances in Biomass Autothermal/Oxidative Pyrolysis: A Review. *ACS Sustain. Chem. Eng*. 2020. **8**: 11888.
41. Gao G., Zhang S., Gao A., Li C., Zhang L., Gao W., Ding K., Huang Y., Gholizadeh M., Hu X. Oxidative Pyrolysis of Poplar Sawdust: Probing the Influence of Oxidation Reactions on Property of Biochar. *J. Energy Inst*. 2024. **115**: 101624.
42. Vuppaladadiyam A.K., Vuppaladadiyam S.S.V., Awasthi A., Sahoo A., Rehman S., Pant K.K., Murugavelh S., Huang Q., Anthony E., Fennel P., Bhattacharya S., Leu Sh.-Yu. Biomass Pyrolysis: A Review on Recent Advancements and Green Hydrogen Production. *Bioresour. Technol*. 2022. **364**: 128087.
43. El Abdellaoui F., Roethlisberger R.P., Ez-Zahraouy H. Oxidative Pyrolysis of Pellets from Lignocellulosic Anaerobic Digestion Residues and Wood Chips for Biochar and Syngas Production. *Fuel.* 2023. **350**: 128824.
44. Gianfelice G., Canu P. On the Mechanism of Single Pellet Smouldering Combustion. *Fuel.* 2021. **301**: 121044.
45. Ohlemiller T. Modeling of smoldering combustion propagation. *Prog. Energ. Combust. Sci*. 1985. **11**(4): 277.
46. Rein G. Smouldering combustion phenomena in science and technology. *Int. Rev. Chem. Eng*. 2009. **1**: 3.
47. Kaltschmitt M., Hartmann H., Hofbauer H. (Editors). *Energie aus Biomasse: Grundlagen, Techniken und Verfahren*. (Berlin/Heidelberg, Germany: Springer, 2016).
48. Milhé M., Van De Steene L., Haube M., Commandré J.M., Fassinou W.F., Flamant G. Autothermal and allothermal pyrolysis in a continuous fixed bed reactor. *J. Anal. Appl. Pyrolysis.* 2013. **103**(SI): 102.
49. Porteiro J., Patiño D., Collazo J., Granada E., Moran J., Miguez J.L. Experimental Analysis of the Ignition Front Propagation of Several Biomass Fuels in a Fixed-Bed Combustor. *Fuel.* 2010, **89**: 26.
50. Porteiro J., Patiño D., Miguez J.L., Granada E., Moran J., Collazo J. Study of the Reaction Front Thickness in a Counter-Current Fixed-Bed Combustor of a Pelletised Biomass. *Combust. Flame.* 2012, **159**: 1296.
51. Pham X.H. *Pyrolyse oxydative de la biomasse en lit fixe. Thèse de doctorat en philosophie.* (Montpellier, France: L'école Doctorale Energie et Environnement, Presses universitaires de Perpignan, 2018).
52. Daouk E., Van De Steene L., Paviet F., Martin E., Valette J., Salvador S. Oxidative Pyrolysis of Wood Chips and of Wood Pellets in a Downdraft Continuous Fixed Bed Reactor. *Fuel.* 2017. **196**: 408.
53. Rizzo A.M., Pettorali M., Nistri R., Chiaramonti D. Mass and Energy Balances of an Autothermal Pilot Carbonization Unit. *Biomass Bioenergy.* 2019. **120**: 144.
54. Reed T.B., Das A. *Handbook of Biomass Downdraft Gasifier Engine System*. (Golden, CO, U.S.: Solar Energy Research Institute/The Biomass Energy Foundation Press, 1988).
55. Basu P. *Biomass Gasification, Pyrolysis, and Torrefaction: Practical Design and Theory*. 2nd ed. (Amsterdam, The Netherlands: Academic Press, 2013).

56. Kaltschmitt M., Hofbauer H., Lenz V. (Eds.) *Energie aus Biomasse: Thermo-Chemische Konversion, Energie aus Biomasse.* (Wiesbaden, Germany: Springer Fachmedien, 2024).
57. Amalina F., Razak A.S.A., Krishnan S., Zularisam A.W., Nasrullah M. A comprehensive assessment of the method for producing biochar, its characterization, stability, and potential applications in regenerative economic sustainability - a review. *Clean Mater*. 2022. **3**: 100045.
58. McKendry P. Energy production from biomass (part 3): gasification technologies. *Bioresour. Technol*. 2002. **83**: 55.
59. Anca-Couce A. Reaction mechanisms and multi-scale modelling of lignocellulosic biomass pyrolysis. *Prog. Energy Combust. Sci*. 2016. **53**: 41.
60. Scholz S.B., Sembres T., Roberts K., Whitman T., Wilson K., Lehmann J. *Biochar Systems for Smallholders in Developing Countries: Leveraging Current Knowledge and Exploring Future Potential for Climate-Smart Agriculture*. (Washington, DC: World Bank Publications, 2014).
61. *Biochar-Producing Stoves to Benefit Climate, Health, and Soil*. (Norfolk: International Biochar Initiative, 2025).
62. *CarbonTerra – carbon-neutral food production with technology solutions for farmers that simplifies the monetization of carbon offsets*. (Saskatchewan, Ca.: Carbonterra, 2021).
63. Shackley C.S. *Biochar Stoves: an innovation studies perspective*. (Edinburgh: UK Biochar Research Centre, School of GeoSciences, University of Edinburgh, 2011).
64. Klyus V., Lobunets Yu., Zurian O., Chetveryk H., Masliukova Z. Pyrolysis furnace of continuous combustion. *Vidnovluvana Energetika*. 2024. **79**(4): 145. [in Ukrainian].
65. Borysenko M.V., Borysenko L.I., Klius V.P., Klius S.V., Shynkarenko V.I. Pyrolysis regeneration of activated carbon used for glycerin purification. *Surface.* 2022. **14(29)**: 95.
66. ASTM International. D-5142, Standard Test Methods for Proximate Analysis of the Analysis Sample of Coal and Coke by Instrumental Procedures. (West Conshohocken: ASTM International, 2009).
67. ASTM International. D-6556-2017, Standard Test Method for Carbon Black − Total and External Surface Area by Nitrogen Adsorption. (West Conshohocken: ASTM International, 2017).
68. ASTM International. D-1513 − 05 (Reapproved 2012), Standard Test Method for Carbon Black, Pelleted - Pour Density. (West Conshohocken: ASTM International, 2012).
69. ASTM International. D-1509 − 18 (Reapproved 2023), Standard Test Methods for Carbon Black—Heating Loss. (West Conshohocken: ASTM International, 2023).
70. ASTM D-1620 − 60 (Reapproved 1969), Standard Method of Test for volatile content of carbon black. (West Conshohocken: ASTM International, 1969).
71. ASTM D-5832 − 98 (Reapproved 2021), Standard Test Method for Volatile Matter Content of Activated Carbon Samples. (West Conshohocken: ASTM International, 2021).
72. ASTM D1762-84 (Reapproved 2021), Standard Test Method for Chemical Analysis of Wood Charcoal. (West Conshohocken: ASTM International, 2021).
73. ASTM D-1506 − 15 (Reapproved 2020), Standard Test Methods for Carbon Black–Ash Content. (West Conshohocken: ASTM International, 2020).
74. Mott R.A., Wilkinson H.C. The use of the Eschka method for the determination of high sulphur contents. *J. Appl. Chem*. 2007. **3**(5): 218.
75. Li X., Liu H., Liu N., Sun Z., Fu S., Zhan X., Yang J., Zhou R., Zhang H., Zhang J., Han X. Pyrolysis temperature had effects on the physicochemical properties of biochar. *Plant Soil Environ*. 2023. **69**(8): 363.
76. He M., Xu Z., Sun Y., Chan P.S., Lui I., Tsang D.C.W. Critical impacts of pyrolysis conditions and activation methods on application-oriented production of wood waste-derived biochar. *Bioresour. Technol*. 2021. **341**: 125811.
77. Khater El-S., Bahnasawy A., Hamouda R., Sabahy A., Abbas W., Morsy O.M. Biochar production under different pyrolysis temperatures with different types of agricultural wastes. *Sci. Rep*. 2024. **14**: 2625.
78. Ghorbani M., Amirahmadi E., Neugschwandtner R.W., Konvalina P., Kopecký M., Moudrý J., Perná K., Murindangabo Y.T. The Impact of Pyrolysis Temperature on Biochar Properties and Its Effects on Soil Hydrological Properties. *Sustainability*. 2022. **14**(22): 14722.
79. Li Y., Gupta R., Zhang Q., You S. Review of biochar production via crop residue pyrolysis: Development and perspectives. *Bioresour. Technol*. 2023. **369**: 128423.
80. Mimmo T., Panzacchi P., Baratieri M., Davies C.A., Tonon G. Effect of pyrolysis temperature on miscanthus (Miscanthus × giganteus) biochar physical, chemical and functional properties. *Biomass Bioenergy*. 2014. **62**: 149.
81. Budai A., Wang L., Gronli M., Strand L.T., Antal Jr. M.J., Abiven S., Dieguez-Alonso A., Anca-Couce A., Rasse D.P. Surface Properties and Chemical Composition of Corncob and Miscanthus Biochars: Effects of Production Temperature and Method. *J. Agric. Food Chem*. 2014. **62**(17): 3791.

82. Klemencova K., Grycova B., Lestinsky P. Influence of Miscanthus Rhizome Pyrolysis Operating Conditions on Products Properties. *Sustainability.* 2022. **14**(10): 6193.
83. Kim H., Kim J., Kim M., Hyun S., Hyun Moon D. Sorption of sulfathiazole in the soil treated with giant Miscanthus-derived biochar: effect of biochar pyrolysis temperature, soil pH, and aging period. *Environ. Sci. Pollut. Res*. 2018. **25**: 25681.
84. Collura S., Azambre B., Finqueneisel G., Zimny T., Weber J.V. Miscanthus × giganteus straw and pellets as sustainable fuels: Combustion and emission tests. *Environ. Chem. Lett*. 2006. **4**: 75.
85. Hideno A. Thermal degradation behavior of ball-milled Miscanthus plants and its relationship to enzymatic hydrolysis. *BioRes*. 2018. **13**(3): 6383.
86. Wemer K., Pommer L., Brostrom M. Thermal decomposition of hemicelluloses. *J. Anal. Appl. Pyrol*. 2014. **110**: 130.
87. Sebio-Puñal T., Naya S., López-Beceiro J., Tarrío-Saavedra J., Artiaga R. Thermogravimetric analysis of wood, holocellulose, and lignin from five wood species. *J. Thermal Anal. Calorim*. 2012. **109**: 1163.
88. Jayaraman K., Gökalp I. Pyrolysis, combustion and gasification characteristics of miscanthus and sewage sludge. *Energy Conv. Manag*. 2015. **89**: 83.
89. Grishchenko L.M., Zhytnyk D.O., Matushko I.P., Diyuk V.E., Noskov Y.V., Malyshev V.Y., Moiseienko V.A., Boldyrieva O.Y., Lisnyak V.V. Microwave Properties of Composite Films Based on Polyvinyl Chloride and Brominated Activated Carbon. *ChemistrySelect*. 2024. **9**: e202400432.
90. Li S., Chen G. Thermogravimetric, thermochemical, and infrared spectral characterization of feedstocks and biochar derived at different pyrolysis temperatures. *Waste Manag*. 2018. **78**: 198.
91. Yang H., Yan R., Chen H., Lee D.H., Zheng C. Characteristics of hemicellulose. cellulose and lignin pyrolysis. *Fuel.* 2007. **86**: 1781.
92. Behazin E., Ogunsona E., Rodriguez-Uribe A., Mohanty A.K., Misra M., Anyia A.O. Mechanical, chemical, and physical properties of wood and perennial grass biochars for possible composite application. *BioRes*. 2016. **11**(1): 1334.
93. de Jesus Duarte S., Glaser B., Paiva de Lima R., Cerri P.C.E. Chemical, Physical, and Hydraulic Properties as Affected by One Year of Miscanthus Biochar Interaction with Sandy and Loamy Tropical Soils. *Soil Syst*. 2019. **3**: 24.
94. Cibati A., Foereid B., Bissessur A., Hapca S. Assessment of *Miscanthus × giganteus* derived biochar as copper and zinc adsorbent: Study of the effect of pyrolysis temperature, pH and hydrogen peroxide modification. *J. Clean. Prod*. 2017. **162**: 1285.
95. Jeguirim M., Limousy L. *Char and carbon materials derived from biomass: production, characterization and applications*. (Amsterdam: Elsevier, 2019).
96. Wiedner K., Rumpel C., Steiner C., Pozzi A., Maas R., Glaser B. Chemical evaluation of chars produced by thermochemical conversion (gasification, pyrolysis and hydrothermal carbonization) of agro-industrial biomass on a commercial scale. *Biomass Bioenergy*. 2013. **59**: 264.
97. Garlapalli R.K., Wirth B., Reza M.T. Pyrolysis of hydrochar from digestate: effect of hydrothermal carbonization and pyrolysis temperatures on pyrochar formation. *Bioresour. Technol*. 2016. **220**: 168.
98. Fahad S., Danish S., Datta R., Saud S., Lichtfouse E. (Editors). *Sustainable Agriculture Reviews 61. Biochar to Improve Crop Production and Decrease Plant Stress under a Changing Climate, Sustainable Agriculture Reviews.* V. 61. (Switzerland, Cham: Springer, 2023).
99. Tag A.T., Duman G., Ucar S., Yanik J. Effects of feedstock type and pyrolysis temperature on potential applications of biochar. *J. Anal. Appl. Pyrol.* 2016. **120**: 200.
100. Mikajlo I., Lerch T.Z., Louvel B., Hynšt J., Záhora J., Pourrut B. Composted biochar versus compost with biochar: effects on soil properties and plant growth. *Biochar*. 2024. **6**: 85.

Received 11.03.2025, accepted 04.09.2025